

Evidence of the $h_c \rightarrow K_S^0 K^+ \pi^- + \text{c.c.}$ decay

M. Ablikim,¹ M. N. Achasov,^{4,c} P. Adlarson,⁷⁵ O. Afedulidis,³ X. C. Ai,⁸⁰ R. Aliberti,³⁵ A. Amoroso,^{74a,74c} Q. An,^{71,58,a} Y. Bai,⁵⁷ O. Bakina,³⁶ I. Balossino,^{29a} Y. Ban,^{46,h} H.-R. Bao,⁶³ V. Batozskaya,^{1,44} K. Begzsuren,³² N. Berger,³⁵ M. Berlowski,⁴⁴ M. Bertani,^{28a} D. Bettoni,^{29a} F. Bianchi,^{74a,74c} E. Bianco,^{74a,74c} A. Bortone,^{74a,74c} I. Boyko,³⁶ R. A. Briere,⁵ A. Brueggemann,⁶⁸ H. Cai,⁷⁶ X. Cai,^{1,58} A. Calcaterra,^{28a} G. F. Cao,^{1,63} N. Cao,^{1,63} S. A. Cetin,^{62a} J. F. Chang,^{1,58} G. R. Che,⁴³ G. Chelkov,^{36,b} C. Chen,⁴³ C. H. Chen,⁹ Chao Chen,⁵⁵ G. Chen,¹ H. S. Chen,^{1,63} H. Y. Chen,²⁰ M. L. Chen,^{1,58,63} S. J. Chen,⁴² S. L. Chen,⁴⁵ S. M. Chen,⁶¹ T. Chen,^{1,63} X. R. Chen,^{31,63} X. T. Chen,^{1,63} Y. B. Chen,^{1,58} Y. Q. Chen,³⁴ Z. J. Chen,^{25,i} Z. Y. Chen,^{1,63} S. K. Choi,¹⁰ G. Cibinetto,^{29a} F. Cossio,^{74c} J. J. Cui,⁵⁰ H. L. Dai,^{1,58} J. P. Dai,⁷⁸ A. Dbeyssi,¹⁸ R. E. de Boer,³ D. Dedovich,³⁶ C. Q. Deng,⁷² Z. Y. Deng,¹ A. Denig,³⁵ I. Denysenko,³⁶ M. Destefanis,^{74a,74c} F. De Mori,^{74a,74c} B. Ding,^{66,1} X. X. Ding,^{46,h} Y. Ding,⁴⁰ Y. Ding,³⁴ J. Dong,^{1,58} L. Y. Dong,^{1,63} M. Y. Dong,^{1,58,63} X. Dong,⁷⁶ M. C. Du,¹ S. X. Du,⁸⁰ Y. Y. Duan,⁵⁵ Z. H. Duan,⁴² P. Egorov,^{36,b} Y. H. Fan,⁴⁵ J. Fang,⁵⁹ J. Fang,^{1,58} S. S. Fang,^{1,63} W. X. Fang,¹ Y. Fang,¹ Y. Q. Fang,^{1,58} R. Farinelli,^{29a} L. Fava,^{74b,74c} F. Feldbauer,³ G. Felici,^{28a} C. Q. Feng,^{71,58} J. H. Feng,⁵⁹ Y. T. Feng,^{71,58} M. Fritsch,³ C. D. Fu,¹ J. L. Fu,⁶³ Y. W. Fu,^{1,63} H. Gao,⁶³ X. B. Gao,⁴¹ Y. N. Gao,^{46,h} Yang Gao,^{71,58} S. Garbolino,^{74c} I. Garzia,^{29a,29b} L. Ge,⁸⁰ P. T. Ge,⁷⁶ Z. W. Ge,⁴² C. Geng,⁵⁹ E. M. Gersabeck,⁶⁷ A. Gilman,⁶⁹ K. Goetzen,¹³ L. Gong,⁴⁰ W. X. Gong,^{1,58} W. Gradl,³⁵ S. Gramigna,^{29a,29b} M. Greco,^{74a,74c} M. H. Gu,^{1,58} Y. T. Gu,¹⁵ C. Y. Guan,^{1,63} A. Q. Guo,^{31,63} L. B. Guo,⁴¹ M. J. Guo,⁵⁰ R. P. Guo,⁴⁹ Y. P. Guo,^{12,g} A. Guskov,^{36,b} J. Gutierrez,²⁷ K. L. Han,⁶³ T. T. Han,¹ F. Hanisch,³ X. Q. Hao,¹⁹ F. A. Harris,⁶⁵ K. K. He,⁵⁵ K. L. He,^{1,63} F. H. Heinsius,³ C. H. Heinz,³⁵ Y. K. Heng,^{1,58,63} C. Herold,⁶⁰ T. Holtmann,³ P. C. Hong,³⁴ G. Y. Hou,^{1,63} X. T. Hou,^{1,63} Y. R. Hou,⁶³ Z. L. Hou,¹ B. Y. Hu,⁵⁹ H. M. Hu,^{1,63} J. F. Hu,^{56,j} S. L. Hu,^{12,g} T. Hu,^{1,58,63} Y. Hu,¹ G. S. Huang,^{71,58} K. X. Huang,⁵⁹ L. Q. Huang,^{31,63} X. T. Huang,⁵⁰ Y. P. Huang,¹ Y. S. Huang,⁵⁹ T. Hussain,⁷³ F. Hölzken,³ N. Hüsken,³⁵ N. in der Wiesche,⁶⁸ J. Jackson,²⁷ S. Janchiv,³² J. H. Jeong,¹⁰ Q. Ji,¹ Q. P. Ji,¹⁹ W. Ji,^{1,63} X. B. Ji,^{1,63} X. L. Ji,^{1,58} Y. Y. Ji,⁵⁰ X. Q. Jia,⁵⁰ Z. K. Jia,^{71,58} D. Jiang,^{1,63} H. B. Jiang,⁷⁶ P. C. Jiang,^{46,h} S. S. Jiang,³⁹ T. J. Jiang,¹⁶ X. S. Jiang,^{1,58,63} Y. Jiang,⁶³ J. B. Jiao,⁵⁰ J. K. Jiao,³⁴ Z. Jiao,²³ S. Jin,⁴² Y. Jin,⁶⁶ M. Q. Jing,^{1,63} X. M. Jing,⁶³ T. Johansson,⁷⁵ S. Kabana,³³ N. Kalantar-Nayestanaki,⁶⁴ X. L. Kang,⁹ X. S. Kang,⁴⁰ M. Kavatsyuk,⁶⁴ B. C. Ke,⁸⁰ V. Khachatryan,²⁷ A. Khoukaz,⁶⁸ R. Kiuchi,¹ O. B. Kolcu,^{62a} B. Kopf,³ M. Kuessner,³ X. Kui,^{1,63} N. Kumar,²⁶ A. Kupsc,^{44,75} W. Kühn,³⁷ J. J. Lane,⁶⁷ P. Larin,¹⁸ L. Lavezzi,^{74a,74c} T. T. Lei,^{71,58} Z. H. Lei,^{71,58} M. Lellmann,³⁵ T. Lenz,³⁵ C. Li,⁴³ C. Li,⁴⁷ C. H. Li,³⁹ Cheng Li,^{71,58} D. M. Li,⁸⁰ F. Li,^{1,58} G. Li,¹ H. B. Li,^{1,63} H. J. Li,¹⁹ H. N. Li,^{56,j} Hui Li,⁴³ J. R. Li,⁶¹ J. S. Li,⁵⁹ K. Li,¹ L. J. Li,^{1,63} L. K. Li,¹ Lei Li,⁴⁸ M. H. Li,⁴³ P. R. Li,^{38,k,l} Q. M. Li,^{1,63} Q. X. Li,⁵⁰ R. Li,^{17,31} S. X. Li,¹² T. Li,⁵⁰ W. D. Li,^{1,63} W. G. Li,^{1,a} X. Li,^{1,63} X. H. Li,^{71,58} X. L. Li,⁵⁰ X. Y. Li,^{1,63} X. Z. Li,⁵⁹ Y. G. Li,^{46,h} Z. J. Li,⁵⁹ Z. Y. Li,⁷⁸ C. Liang,⁴² H. Liang,^{1,63} H. Liang,^{71,58} Y. F. Liang,⁵⁴ Y. T. Liang,^{31,63} G. R. Liao,¹⁴ L. Z. Liao,⁵⁰ Y. P. Liao,^{1,63} J. Libby,²⁶ A. Limphirat,⁶⁰ C. C. Lin,⁵⁵ D. X. Lin,^{31,63} T. Lin,¹ B. J. Liu,¹ B. X. Liu,⁷⁶ C. Liu,³⁴ C. X. Liu,¹ F. Liu,¹ F. H. Liu,⁵³ Feng Liu,⁶ G. M. Liu,^{56,j} H. Liu,^{38,k,l} H. B. Liu,¹⁵ H. H. Liu,¹ H. M. Liu,^{1,63} Huihui Liu,²¹ J. B. Liu,^{71,58} J. Y. Liu,^{1,63} K. Liu,^{38,k,l} K. Y. Liu,⁴⁰ Ke Liu,²² L. Liu,^{71,58} L. C. Liu,⁴³ Lu Liu,⁴³ M. H. Liu,^{12,g} P. L. Liu,¹ Q. Liu,⁶³ S. B. Liu,^{71,58} T. Liu,^{12,g} W. K. Liu,⁴³ W. M. Liu,^{71,58} X. Liu,^{38,k,l} X. Liu,³⁹ Y. Liu,⁸⁰ Y. Liu,^{38,k,l} Y. B. Liu,⁴³ Z. A. Liu,^{1,58,63} Z. D. Liu,⁹ Z. Q. Liu,⁵⁰ X. C. Lou,^{1,58,63} F. X. Lu,⁵⁹ H. J. Lu,²³ J. G. Lu,^{1,58} X. L. Lu,¹ Y. Lu,⁷ Y. P. Lu,^{1,58} Z. H. Lu,^{1,63} C. L. Luo,⁴¹ J. R. Luo,⁵⁹ M. X. Luo,⁷⁹ T. Luo,^{12,g} X. L. Luo,^{1,58} X. R. Lyu,⁶³ Y. F. Lyu,⁴³ F. C. Ma,⁴⁰ H. Ma,⁷⁸ H. L. Ma,¹ J. L. Ma,^{1,63} L. L. Ma,⁵⁰ M. M. Ma,^{1,63} Q. M. Ma,¹ R. Q. Ma,^{1,63} T. Ma,^{71,58} X. T. Ma,^{1,63} X. Y. Ma,^{1,58} Y. Ma,^{46,h} Y. M. Ma,³¹ F. E. Maas,¹⁸ M. Maggiora,^{74a,74c} S. Malde,⁶⁹ Y. J. Mao,^{46,h} Z. P. Mao,¹ S. Marcello,^{74a,74c} Z. X. Meng,⁶⁶ J. G. Messchendorp,^{13,64} G. Mezzadri,^{29a} H. Miao,^{1,63} T. J. Min,⁴² R. E. Mitchell,²⁷ X. H. Mo,^{1,58,63} B. Moses,²⁷ N. Yu. Muchnoi,^{4,c} J. Muskalla,³⁵ Y. Nefedov,³⁶ F. Nerling,^{18,e} L. S. Nie,²⁰ I. B. Nikolaev,^{4,c} Z. Ning,^{1,58} S. Nisar,^{11,m} Q. L. Niu,^{38,k,l} W. D. Niu,⁵⁵ Y. Niu,⁵⁰ S. L. Olsen,⁶³ Q. Ouyang,^{1,58,63} S. Pacetti,^{28b,28c} X. Pan,⁵⁵ Y. Pan,⁵⁷ A. Pathak,³⁴ P. Patteri,^{28a} Y. P. Pei,^{71,58} M. Pelizaeus,³ H. P. Peng,^{71,58} Y. Y. Peng,^{38,k,l} K. Peters,^{13,e} J. L. Ping,⁴¹ R. G. Ping,^{1,63} S. Plura,³⁵ V. Prasad,³³ F. Z. Qi,¹ H. Qi,^{71,58} H. R. Qi,⁶¹ M. Qi,⁴² T. Y. Qi,^{12,g} S. Qian,^{1,58} W. B. Qian,⁶³ C. F. Qiao,⁶³ X. K. Qiao,⁸⁰ J. J. Qin,⁷² L. Q. Qin,¹⁴ L. Y. Qin,^{71,58} X. S. Qin,⁵⁰ Z. H. Qin,^{1,58} J. F. Qiu,¹ Z. H. Qu,⁷² C. F. Redmer,³⁵ K. J. Ren,³⁹ A. Rivetti,^{74c} M. Rolo,^{74c} G. Rong,^{1,63} Ch. Rosner,¹⁸ S. N. Ruan,⁴³ N. Salone,⁴⁴ A. Sarantsev,^{36,d} Y. Schelhaas,³⁵ K. Schoenning,⁷⁵ M. Scodreggio,^{29a} K. Y. Shan,^{12,g} W. Shan,²⁴ X. Y. Shan,^{71,58} Z. J. Shang,^{38,k,l} J. F. Shanguan,¹⁶ L. G. Shao,^{1,63} M. Shao,^{71,58} C. P. Shen,^{12,g} H. F. Shen,^{1,8} W. H. Shen,⁶³ X. Y. Shen,^{1,63} B. A. Shi,⁶³ H. Shi,^{71,58} H. C. Shi,^{71,58} J. L. Shi,^{12,g} J. Y. Shi,¹ Q. Q. Shi,⁵⁵ S. Y. Shi,⁷² X. Shi,^{1,58} J. J. Song,¹⁹ T. Z. Song,⁵⁹ W. M. Song,^{34,1} Y. J. Song,^{12,g} Y. X. Song,^{46,h,n} S. Sosio,^{74a,74c} S. Spataro,^{74a,74c} F. Stieler,³⁵ Y. J. Su,⁶³ G. B. Sun,⁷⁶ G. X. Sun,¹ H. Sun,⁶³ H. K. Sun,¹ J. F. Sun,¹⁹ K. Sun,⁶¹ L. Sun,⁷⁶ S. S. Sun,^{1,63} T. Sun,^{51,f} W. Y. Sun,³⁴ Y. Sun,⁹ Y. J. Sun,^{71,58} Y. Z. Sun,¹ Z. Q. Sun,^{1,63} Z. T. Sun,⁵⁰ C. J. Tang,⁵⁴ G. Y. Tang,¹ J. Tang,⁵⁹ M. Tang,^{71,58} Y. A. Tang,⁷⁶ L. Y. Tao,⁷² Q. T. Tao,^{25,i} M. Tat,⁶⁹ J. X. Teng,^{71,58} V. Thoren,⁷⁵ W. H. Tian,⁵⁹ Y. Tian,^{31,63} Z. F. Tian,⁷⁶ I. Uman,^{62b} Y. Wan,⁵⁵ S. J. Wang,⁵⁰ B. Wang,¹ B. L. Wang,⁶³ Bo Wang,^{71,58} D. Y. Wang,^{46,h} F. Wang,⁷² H. J. Wang,^{38,k,l} J. J. Wang,⁷⁶ J. P. Wang,⁵⁰ K. Wang,^{1,58}


L. L. Wang,¹ M. Wang,⁵⁰ N. Y. Wang,⁶³ S. Wang,^{12,g} S. Wang,^{38,k,l} T. Wang,^{12,g} T. J. Wang,⁴³ W. Wang,⁷² W. Wang,⁵⁹
W. P. Wang,^{35,71,o} X. Wang,^{46,h} X. F. Wang,^{38,k,l} X. J. Wang,³⁹ X. L. Wang,^{12,g} X. N. Wang,¹ Y. Wang,⁶¹ Y. D. Wang,⁴⁵
Y. F. Wang,^{1,58,63} Y. L. Wang,¹⁹ Y. N. Wang,⁴⁵ Y. Q. Wang,¹ Yaqian Wang,¹⁷ Yi Wang,⁶¹ Z. Wang,^{1,58} Z. L. Wang,⁷²
Z. Y. Wang,^{1,63} Ziyi Wang,⁶³ D. H. Wei,¹⁴ F. Weidner,⁶⁸ S. P. Wen,¹ Y. R. Wen,³⁹ U. Wiedner,³ G. Wilkinson,⁶⁹ M. Wolke,⁷⁵
L. Wollenberg,³ C. Wu,³⁹ J. F. Wu,^{1,8} L. H. Wu,¹ L. J. Wu,^{1,63} X. Wu,^{12,g} X. H. Wu,³⁴ Y. Wu,^{71,58} Y. H. Wu,⁵⁵ Y. J. Wu,³¹
Z. Wu,^{1,58} L. Xia,^{71,58} X. M. Xian,³⁹ B. H. Xiang,^{1,63} T. Xiang,^{46,h} D. Xiao,^{38,k,l} G. Y. Xiao,⁴² S. Y. Xiao,¹ Y. L. Xiao,^{12,g}
Z. J. Xiao,⁴¹ C. Xie,⁴² X. H. Xie,^{46,h} Y. Xie,⁵⁰ Y. G. Xie,^{1,58} Y. H. Xie,⁶ Z. P. Xie,^{71,58} T. Y. Xing,^{1,63} C. F. Xu,^{1,63} C. J. Xu,⁵⁹
G. F. Xu,¹ H. Y. Xu,^{66,2,p} M. Xu,^{71,58} Q. J. Xu,¹⁶ Q. N. Xu,³⁰ W. Xu,¹ W. L. Xu,⁶⁶ X. P. Xu,⁵⁵ Y. C. Xu,⁷⁷ Z. P. Xu,⁴²
Z. S. Xu,⁶³ F. Yan,^{12,g} L. Yan,^{12,g} W. B. Yan,^{71,58} W. C. Yan,⁸⁰ X. Q. Yan,¹ H. J. Yang,^{51,f} H. L. Yang,³⁴ H. X. Yang,¹
T. Yang,¹ Y. Yang,^{12,g} Y. F. Yang,⁴³ Y. F. Yang,^{1,63} Y. X. Yang,^{1,63} Z. W. Yang,^{38,k,l} Z. P. Yao,⁵⁰ M. Ye,^{1,58} M. H. Ye,⁸
J. H. Yin,¹ Z. Y. You,⁵⁹ B. X. Yu,^{1,58,63} C. X. Yu,⁴³ G. Yu,^{1,63} J. S. Yu,^{25,i} T. Yu,⁷² X. D. Yu,^{46,h} Y. C. Yu,⁸⁰ C. Z. Yuan,^{1,63}
J. Yuan,⁴⁵ J. Yuan,³⁴ L. Yuan,² S. C. Yuan,^{1,63} Y. Yuan,^{1,63} Z. Y. Yuan,⁵⁹ C. X. Yue,³⁹ A. A. Zafar,⁷³ F. R. Zeng,⁵⁰
S. H. Zeng,⁷² X. Zeng,^{12,g} Y. Zeng,^{25,i} Y. J. Zeng,^{1,63} Y. J. Zeng,⁵⁹ X. Y. Zhai,³⁴ Y. C. Zhai,⁵⁰ Y. H. Zhan,⁵⁹ A. Q. Zhang,^{1,63}
B. L. Zhang,^{1,63} B. X. Zhang,¹ D. H. Zhang,⁴³ G. Y. Zhang,¹⁹ H. Zhang,⁸⁰ H. Zhang,^{71,58} H. C. Zhang,^{1,58,63} H. H. Zhang,⁵⁹
H. H. Zhang,³⁴ H. Q. Zhang,^{1,58,63} H. R. Zhang,^{71,58} H. Y. Zhang,^{1,58} J. Zhang,⁸⁰ J. Zhang,⁵⁹ J. J. Zhang,⁵² J. L. Zhang,²⁰
J. Q. Zhang,⁴¹ J. S. Zhang,^{12,g} J. W. Zhang,^{1,58,63} J. X. Zhang,^{38,k,l} J. Y. Zhang,¹ J. Z. Zhang,^{1,63} Jianyu Zhang,⁶³
L. M. Zhang,⁶¹ Lei Zhang,⁴² P. Zhang,^{1,63} Q. Y. Zhang,³⁴ R. Y. Zhang,^{38,k,l} S. H. Zhang,^{1,63} Shulei Zhang,^{25,i} X. D. Zhang,⁴⁵
X. M. Zhang,¹ X. Y. Zhang,⁵⁰ Y. Zhang,⁷² Y. Zhang,¹ Y. T. Zhang,⁸⁰ Y. H. Zhang,^{1,58} Y. M. Zhang,³⁹ Yan Zhang,^{71,58}
Z. D. Zhang,¹ Z. H. Zhang,¹ Z. L. Zhang,³⁴ Z. Y. Zhang,⁴³ Z. Y. Zhang,⁷⁶ Z. Z. Zhang,⁴⁵ G. Zhao,¹ J. Y. Zhao,^{1,63}
J. Z. Zhao,^{1,58} L. Zhao,¹ Lei Zhao,^{71,58} M. G. Zhao,⁴³ N. Zhao,⁷⁸ R. P. Zhao,⁶³ S. J. Zhao,⁸⁰ Y. B. Zhao,^{1,58} Y. X. Zhao,^{31,63}
Z. G. Zhao,^{71,58} A. Zhemchugov,^{36,b} B. Zheng,⁷² B. M. Zheng,³⁴ J. P. Zheng,^{1,58} W. J. Zheng,^{1,63} Y. H. Zheng,⁶³ B. Zhong,⁴¹
X. Zhong,⁵⁹ H. Zhou,⁵⁰ J. Y. Zhou,³⁴ L. P. Zhou,^{1,63} S. Zhou,⁶ X. Zhou,⁷⁶ X. K. Zhou,⁶ X. R. Zhou,^{71,58} X. Y. Zhou,³⁹
Y. Z. Zhou,^{12,g} J. Zhu,⁴³ K. Zhu,¹ K. J. Zhu,^{1,58,63} K. S. Zhu,^{12,g} L. Zhu,³⁴ L. X. Zhu,⁶³ S. H. Zhu,⁷⁰ S. Q. Zhu,⁴² T. J. Zhu,^{12,g}
W. D. Zhu,⁴¹ Y. C. Zhu,^{71,58} Z. A. Zhu,^{1,63} J. H. Zou,¹ and J. Zu^{71,58}

(BESIII Collaboration)

¹*Institute of High Energy Physics, Beijing 100049, People's Republic of China*²*Beihang University, Beijing 100191, People's Republic of China*³*Bochum Ruhr-University, D-44780 Bochum, Germany*⁴*Budker Institute of Nuclear Physics SB RAS (BINP), Novosibirsk 630090, Russia*⁵*Carnegie Mellon University, Pittsburgh, Pennsylvania 15213, USA*⁶*Central China Normal University, Wuhan 430079, People's Republic of China*⁷*Central South University, Changsha 410083, People's Republic of China*⁸*China Center of Advanced Science and Technology, Beijing 100190, People's Republic of China*⁹*China University of Geosciences, Wuhan 430074, People's Republic of China*¹⁰*Chung-Ang University, Seoul, 06974, Republic of Korea*¹¹*COMSATS University Islamabad, Lahore Campus, Defence Road, Off Raiwind Road, 54000 Lahore, Pakistan*¹²*Fudan University, Shanghai 200433, People's Republic of China*¹³*GSI Helmholtzcentre for Heavy Ion Research GmbH, D-64291 Darmstadt, Germany*¹⁴*Guangxi Normal University, Guilin 541004, People's Republic of China*¹⁵*Guangxi University, Nanning 530004, People's Republic of China*¹⁶*Hangzhou Normal University, Hangzhou 310036, People's Republic of China*¹⁷*Hebei University, Baoding 071002, People's Republic of China*¹⁸*Helmholtz Institute Mainz, Staudinger Weg 18, D-55099 Mainz, Germany*¹⁹*Henan Normal University, Xinxiang 453007, People's Republic of China*²⁰*Henan University, Kaifeng 475004, People's Republic of China*²¹*Henan University of Science and Technology, Luoyang 471003, People's Republic of China*²²*Henan University of Technology, Zhengzhou 450001, People's Republic of China*²³*Huangshan College, Huangshan 245000, People's Republic of China*²⁴*Hunan Normal University, Changsha 410081, People's Republic of China*²⁵*Hunan University, Changsha 410082, People's Republic of China*²⁶*Indian Institute of Technology Madras, Chennai 600036, India*²⁷*Indiana University, Bloomington, Indiana 47405, USA*^{28a}*INFN Laboratori Nazionali di Frascati, I-00044, Frascati, Italy*

- ^{28b}INFN Sezione di Perugia, I-06100, Perugia, Italy
^{28c}University of Perugia, I-06100, Perugia, Italy
^{29a}INFN Sezione di Ferrara, I-44122, Ferrara, Italy
^{29b}University of Ferrara, I-44122, Ferrara, Italy
³⁰Inner Mongolia University, Hohhot 010021, People's Republic of China
³¹Institute of Modern Physics, Lanzhou 730000, People's Republic of China
³²Institute of Physics and Technology, Peace Avenue 54B, Ulaanbaatar 13330, Mongolia
³³Instituto de Alta Investigación, Universidad de Tarapacá, Casilla 7D, Arica 1000000, Chile
³⁴Jilin University, Changchun 130012, People's Republic of China
³⁵Johannes Gutenberg University of Mainz, Johann-Joachim-Becher-Weg 45, D-55099 Mainz, Germany
³⁶Joint Institute for Nuclear Research, 141980 Dubna, Moscow Region, Russia
³⁷Justus-Liebig-Universitaet Giessen, II. Physikalisches Institut, Heinrich-Buff-Ring 16, D-35392 Giessen, Germany
³⁸Lanzhou University, Lanzhou 730000, People's Republic of China
³⁹Liaoning Normal University, Dalian 116029, People's Republic of China
⁴⁰Liaoning University, Shenyang 110036, People's Republic of China
⁴¹Nanjing Normal University, Nanjing 210023, People's Republic of China
⁴²Nanjing University, Nanjing 210093, People's Republic of China
⁴³Nankai University, Tianjin 300071, People's Republic of China
⁴⁴National Centre for Nuclear Research, Warsaw 02-093, Poland
⁴⁵North China Electric Power University, Beijing 102206, People's Republic of China
⁴⁶Peking University, Beijing 100871, People's Republic of China
⁴⁷Qufu Normal University, Qufu 273165, People's Republic of China
⁴⁸Renmin University of China, Beijing 100872, People's Republic of China
⁴⁹Shandong Normal University, Jinan 250014, People's Republic of China
⁵⁰Shandong University, Jinan 250100, People's Republic of China
⁵¹Shanghai Jiao Tong University, Shanghai 200240, People's Republic of China
⁵²Shanxi Normal University, Linfen 041004, People's Republic of China
⁵³Shanxi University, Taiyuan 030006, People's Republic of China
⁵⁴Sichuan University, Chengdu 610064, People's Republic of China
⁵⁵Soochow University, Suzhou 215006, People's Republic of China
⁵⁶South China Normal University, Guangzhou 510006, People's Republic of China
⁵⁷Southeast University, Nanjing 211100, People's Republic of China
⁵⁸State Key Laboratory of Particle Detection and Electronics, Beijing 100049, Hefei 230026, People's Republic of China
⁵⁹Sun Yat-Sen University, Guangzhou 510275, People's Republic of China
⁶⁰Suranaree University of Technology, University Avenue 111, Nakhon Ratchasima 30000, Thailand
⁶¹Tsinghua University, Beijing 100084, People's Republic of China
^{62a}Turkish Accelerator Center Particle Factory Group, Istinye University, 34010, Istanbul, Turkey
^{62b}Near East University, Nicosia, North Cyprus, 99138, Mersin 10, Turkey
⁶³University of Chinese Academy of Sciences, Beijing 100049, People's Republic of China
⁶⁴University of Groningen, NL-9747 AA Groningen, The Netherlands
⁶⁵University of Hawaii, Honolulu, Hawaii 96822, USA
⁶⁶University of Jinan, Jinan 250022, People's Republic of China
⁶⁷University of Manchester, Oxford Road, Manchester, M13 9PL, United Kingdom
⁶⁸University of Muenster, Wilhelm-Klemm-Strasse 9, 48149 Muenster, Germany
⁶⁹University of Oxford, Keble Road, Oxford OX13RH, United Kingdom
⁷⁰University of Science and Technology Liaoning, Anshan 114051, People's Republic of China
⁷¹University of Science and Technology of China, Hefei 230026, People's Republic of China
⁷²University of South China, Hengyang 421001, People's Republic of China
⁷³University of the Punjab, Lahore-54590, Pakistan
^{74a}University of Turin and INFN, University of Turin, I-10125, Turin, Italy
^{74b}University of Eastern Piedmont, I-15121, Alessandria, Italy
^{74c}INFN, I-10125, Turin, Italy
⁷⁵Uppsala University, Box 516, SE-75120 Uppsala, Sweden
⁷⁶Wuhan University, Wuhan 430072, People's Republic of China
⁷⁷Yantai University, Yantai 264005, People's Republic of China
⁷⁸Yunnan University, Kunming 650500, People's Republic of China

⁷⁹Zhejiang University, Hangzhou 310027, People's Republic of China
⁸⁰Zhengzhou University, Zhengzhou 450001, People's Republic of China

 (Received 7 April 2024; accepted 16 May 2024; published 12 July 2024)

Based on $(2.712 \pm 0.014) \times 10^9$ $\psi(3686)$ events collected by the BESIII Collaboration, evidence of the hadronic decay $h_c \rightarrow K_S^0 K^+ \pi^- + \text{c.c.}$ is found with a significance of 4.3σ in the $\psi(3686) \rightarrow \pi^0 h_c$ process. The branching fraction of $h_c \rightarrow K_S^0 K^+ \pi^- + \text{c.c.}$ is measured to be $(7.3 \pm 1.8 \pm 0.8) \times 10^{-4}$, where the first and second uncertainties are statistical and systematic, respectively. Combining with the exclusive decay width of $\eta_c \rightarrow K \bar{K} \pi$, our result indicates inconsistencies with both pQCD and NRQCD predictions.

DOI: [10.1103/PhysRevD.110.012007](https://doi.org/10.1103/PhysRevD.110.012007)

I. INTRODUCTION

In the framework of the Standard Model, one fundamental assumption is that the strong interaction between quarks is mediated by colored gluons, as described by

quantum chromodynamics (QCD) [1–3]. Since the derivative of the QCD coupling strength (α_s) with respect to the logarithm of the energy scale, i.e., the β function, is negative [1,2], α_s is divergent in the low-energy limit, bringing large uncertainties to the theoretical calculations in this nonperturbative region. Because of their large mass scales and nonrelativistic nature, charmonia are ideal probes to study and understand QCD from both perturbative and nonperturbative aspects. Based on perturbative QCD (pQCD) and nonrelativistic QCD (NRQCD), the branching fractions of several light hadron decay channels of the P -wave spin singlet charmonium $h_c(1P)$ are calculated [4]. For the channel $K \bar{K} \pi$, the predictions are $(1.4 \pm 0.9)\%$ (pQCD) and $(5.5 \pm 3.3)\%$ (NRQCD), respectively. An experimental measurement on this channel is helpful for testing the validity of these approaches.

^aDeceased.

^bAlso at the Moscow Institute of Physics and Technology, Moscow 141700, Russia.

^cAlso at the Novosibirsk State University, Novosibirsk, 630090, Russia.

^dAlso at the NRC “Kurchatov Institute,” PNPI, 188300, Gatchina, Russia.

^eAlso at Goethe University Frankfurt, 60323 Frankfurt am Main, Germany.

^fAlso at Key Laboratory for Particle Physics, Astrophysics and Cosmology, Ministry of Education; Shanghai Key Laboratory for Particle Physics and Cosmology; Institute of Nuclear and Particle Physics, Shanghai 200240, People's Republic of China.

^gAlso at Key Laboratory of Nuclear Physics and Ion-beam Application (MOE) and Institute of Modern Physics, Fudan University, Shanghai 200443, People's Republic of China.

^hAlso at State Key Laboratory of Nuclear Physics and Technology, Peking University, Beijing 100871, People's Republic of China.

ⁱAlso at School of Physics and Electronics, Hunan University, Changsha 410082, China.

^jAlso at Guangdong Provincial Key Laboratory of Nuclear Science, Institute of Quantum Matter, South China Normal University, Guangzhou 510006, China.

^kAlso at MOE Frontiers Science Center for Rare Isotopes, Lanzhou University, Lanzhou 730000, People's Republic of China.

^lAlso at Lanzhou Center for Theoretical Physics, Lanzhou University, Lanzhou 730000, People's Republic of China.

^mAlso at the Department of Mathematical Sciences, IBA, Karachi 75270, Pakistan.

ⁿAlso at Ecole Polytechnique Federale de Lausanne (EPFL), CH-1015 Lausanne, Switzerland.

^oAlso at Helmholtz Institute Mainz, Staudinger Weg 18, D-55099 Mainz, Germany.

^pAlso at School of Physics, Beihang University, Beijing 100191, China.

While many hadronic decay modes of the S -wave charmonia including J/ψ and $\psi(3686)$ have been discovered and determined precisely, the knowledge of the hadronic decays of h_c is still sparse since its direct production via e^+e^- annihilation is forbidden. Until now, only a few hadronic decay modes have been observed [5,6] via the $\psi(3686) \rightarrow \pi^0 h_c$ process, with a sum of branching fractions less than 5% [7]. According to the experimental result on the branching fraction of the prominent electromagnetic transition $\mathcal{B}(h_c \rightarrow \gamma \eta_c) = (57.66_{-3.50}^{+3.62} \pm 0.58)\%$ [8], the fraction of gluonic annihilation width $\mathcal{B}(h_c \rightarrow 3g)$ is estimated to be about 42%, indicating that a significant fraction of h_c hadronic decay modes remain unknown. Furthermore, although the decay $h_c \rightarrow K_S^0 K^+ \pi^-$ has been predicted for a long time [4], it has not yet been discovered; only an upper limit of 6×10^{-4} has been determined [6,7].

A search for the hadronic decay mode $h_c \rightarrow K_S^0 K^+ \pi^-$ is performed based on the $\psi(3686) \rightarrow \pi^0 h_c$ process from the data sample with $(2.712 \pm 0.014) \times 10^9$ $\psi(3686)$ events [9] collected at center-of-mass energy $\sqrt{s} = 3.686$ GeV with the BESIII detector. Throughout this paper, charged conjugation is always implied unless otherwise specified.

Published by the American Physical Society under the terms of the [Creative Commons Attribution 4.0 International license](https://creativecommons.org/licenses/by/4.0/). Further distribution of this work must maintain attribution to the author(s) and the published article's title, journal citation, and DOI. Funded by SCOAP³.

II. BESIII DETECTOR AND MONTE CARLO SIMULATION

The BESIII detector [10] records symmetric e^+e^- collisions provided by the BEPCII storage ring [11], which operates with a center-of-mass energy range from 2.00 to 4.95 GeV, with a peak luminosity of $1.1 \times 10^{33} \text{ cm}^{-2} \text{ s}^{-1}$ achieved at 3.773 GeV. BESIII has collected large data samples in this energy region [12–14]. The cylindrical core of the BESIII detector covers 93% of the full solid angle and consists of a helium-based multilayer drift chamber (MDC), a plastic scintillator time-of-flight system (TOF), and a CsI(Tl) electromagnetic calorimeter (EMC), which are all enclosed in a superconducting solenoidal magnet providing a 1.0 T magnetic field. The solenoid is supported by an octagonal flux-return yoke with resistive plate counter muon-identification modules interleaved with steel. The charged-particle momentum resolution at 1 GeV/c is 0.5%, and the resolution of the rate of energy loss, dE/dx , is 6% for electrons from Bhabha scattering. The EMC measures photon energies with a resolution of 2.5% (5%) at 1 GeV in the barrel (end-cap) region. The time resolution in the TOF barrel region is 68 ps, while that in the end-cap region is 110 ps. The end-cap TOF system was upgraded in 2015 using multigap resistive plate chamber technology, providing a time resolution of 60 ps, which benefits 80% of the data used in this analysis [15–17].

Simulated data samples produced with a Geant4-based [18] Monte Carlo (MC) simulation, which includes the geometric description of the BESIII detector and the detector response, are used to determine detection efficiencies and to estimate backgrounds. The simulation models the beam-energy spread and initial-state radiation in the e^+e^- annihilations with the generator KKMC [19]. The inclusive MC sample includes the production of the $\psi(3686)$ resonance, the ISR production of the J/ψ , and the continuum processes incorporated in KKMC [19]. All particle decays are modeled with EvtGen [20,21] using branching fractions either taken from the Particle Data Group [7], when available, or otherwise estimated with LUNDCHARM [22,23]. Final-state radiation from charged final-state particles is incorporated using PHOTOS [24]. Additionally, an exclusive MC sample of the signal process $\psi(3686) \rightarrow \pi^0 h_c, h_c \rightarrow K_S^0 K^+ \pi^-$ is generated for the selection criteria optimization and detection efficiency determination, where both $\psi(3686) \rightarrow \pi^0 h_c$ and $h_c \rightarrow K_S^0 K^+ \pi^-$ are simulated based on a uniform phase space distribution.

III. DATA ANALYSIS

A. Event selection

To select $\pi^0 K_S^0 K^+ \pi^-$ events, all the charged tracks are required to be within a polar angle (θ) range of $|\cos\theta| < 0.93$, where θ is measured with respect to the z axis, i.e., the symmetry axis of MDC. Exactly four

charged tracks are required after the polar angle selection, and the total net charge is required to be zero.

To reconstruct K_S^0 , all pairs of oppositely charged tracks are subjected to a secondary vertex fit, which constrains the two tracks to originate from a common vertex. The pair with invariant mass closest to the K_S^0 known mass is chosen, and the distance of the common vertex to the interaction point normalized by its uncertainty, $L/\Delta L$, is required to be greater than 2.

For the charged tracks not originating from K_S^0 decays, the distance of closest approach to the interaction point (IP) must be less than 10 cm along the z axis and less than 1 cm in the transverse plane. For each track, particle identification (PID) chi-square values $\chi_{\text{PID}}^2(\mathcal{P}_{\pm})$ under different particle hypotheses are computed utilizing the combined information of dE/dx and TOF, where $\mathcal{P} \in \{K, \pi\}$ refers to the particle types and the subscript indicates the positive or negative charge of the particle.

Photon candidates are reconstructed from electromagnetic clusters produced in the crystals of the EMC. Clusters with deposited energy larger than 25 MeV in the barrel region ($|\cos\theta| < 0.8$) or 50 MeV in the end-cap region ($0.86 < |\cos\theta| < 0.92$) are selected as photon candidates. The EMC timing of each photon counted from the event start time is required to be within $[0, 700]$ ns to suppress noise and energy deposits unrelated to the event. The opening angle between the photon and the nearest charged track in angle is required to be larger than 10° to suppress the showers from charged tracks.

A pair of photons is accepted as a π^0 candidate if their invariant mass falls into the range $(0.12, 0.15) \text{ MeV}/c^2$. At least one π^0 is required. All combinations of final-state particles are subjected to a five-constraint kinematic fit, with the constraints provided by four-momentum conservation and the π^0 mass. PID of the two tracks and the selection of the best π^0 among multiple candidates are accomplished by minimizing $\chi^2 = \chi_{5C}^2 + \chi_{\text{PID}}^2(\mathcal{P}_+) + \chi_{\text{PID}}^2(\mathcal{P}_-)$, where χ_{5C}^2 is the fit quality of the 5C kinematic fit. The combination with the minimum χ^2 satisfying $\mathcal{P}_+ \mathcal{P}_- = K^+ \pi^-$ or $K^- \pi^+$ is accepted as a signal candidate. Additionally, $\chi_{5C}^2 < 124$ is required to further suppress the non- $\pi^0 K_S^0 K^+ \pi^-$ background.

To suppress the background with one more or one less photon in the final state, a four-constraint kinematic fit, with the constraint provided by four-momentum conservation, is performed, and the chi-square values with one or three photons $\chi_{4C}^2(1\gamma)$ and $\chi_{4C}^2(3\gamma)$ are required to be larger than that of the signal candidate, where the test is done for all the photon candidates. Backgrounds π^0 produced from $K^*(892)^+ \rightarrow K^+ \pi^0$ are found in the inclusive MC sample and removed by applying $|M(K^+ \pi^0) - m(K^*(892)^+)| > 10 \text{ MeV}/c^2$, where $M(K^+ \pi^0)$ is the invariant mass of $K^+ \pi^0$ and $m(K^*(892)^+)$ is the known mass of $K^*(892)^+$ [7]. All the selection criteria have

been optimized by maximizing the figure of merit defined in Ref. [25], $\epsilon/(a/2 + \sqrt{B})$, where $a = 5$ is the desired one-tailed significance, ϵ is the selection efficiency, and B is the expected number of background events falling in the signal range from MC simulation. Here, the signal range is defined as $|M(K_S^0 K^+ \pi^-) - m(h_c)| < 6 \text{ MeV}/c^2$, where $M(K_S^0 K^+ \pi^-)$ is the invariant mass of $K_S^0 K^+ \pi^-$, $m(h_c)$ is the h_c known mass [7], and the interval is determined to be about $\pm 2\sigma$ with respect to the resolution ($3.16 \text{ MeV}/c^2$).

B. Fit to data

To determine the number of signal events N , an unbinned maximum-likelihood fit is performed on the $M(K_S^0 K^+ \pi^-)$ distribution, as shown in Fig. 1. In the fit, the h_c signal is modeled by the shape obtained from the signal MC sample convolved with a Gaussian function, which accounts for the difference in the mass resolution between MC simulation and data. The central value and standard deviation of the Gaussian function are fixed to those obtained by studying the control sample of $\psi(3686) \rightarrow \gamma \chi_{c1,c2}, \chi_{c1,c2} \rightarrow K_S^0 K^+ \pi^-$. A peaking background component from $\psi(3686) \rightarrow \gamma \chi_{c2}, \chi_{c2} \rightarrow K_S^0 K^+ \pi^-$ plus a fake photon, which forms a peak at the left side of the h_c signal, is included in the fit. The number of peaking background events is fixed based on the measured branching fraction [7]. Background from other channels distributes smoothly and is described by an ARGUS function [26], with the threshold parameter fixed to the kinematic threshold $3.551 \text{ GeV}/c^2$. The fit gives $N = 205 \pm 50$ with a statistical significance 4.6σ , determined by the likelihood ratio of the fit with and without the h_c signal function [27].

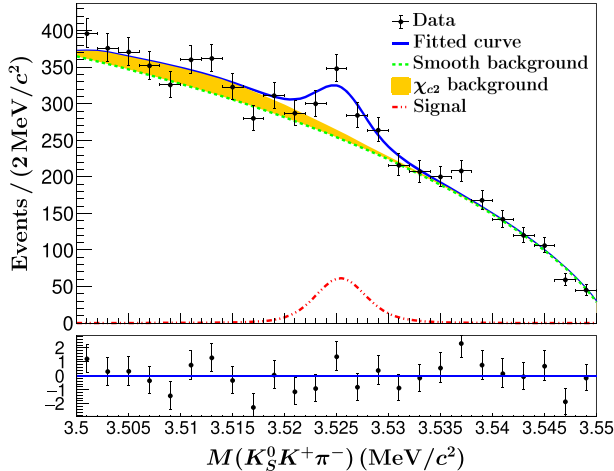


FIG. 1. Fit to the $M(K_S^0 K^+ \pi^-)$ distribution. The black dots with error bars are data, the blue solid curve is the total fit result, the red dashed-dotted curve is the h_c signal, the green dashed curve represents the smooth background, and the orange-filled shape represents the χ_{c2} peaking background.

The branching fraction is calculated with

$$\mathcal{B}(h_c \rightarrow K_S^0 K^+ \pi^-) \times \mathcal{B}(\psi(3686)) = \frac{N}{\epsilon N_{\psi(3686)} \mathcal{B}(K_S^0) \mathcal{B}(\pi^0)}, \quad (1)$$

where $\epsilon = 20.8\%$ is the selection efficiency, $N_{\psi(3686)}$ is the number of $\psi(3686)$ events [9], $\mathcal{B}(K_S^0)$ and $\mathcal{B}(\pi^0)$ are the branching fractions of $K_S^0 \rightarrow \pi^+ \pi^-$ and $\pi^0 \rightarrow \gamma \gamma$, respectively, from the Particle Data Group [7], and $\mathcal{B}(\psi(3686))$ is the branching fraction of $\psi(3686) \rightarrow \pi^0 h_c$ from Ref. [8]. The resulting values are $\mathcal{B}(h_c \rightarrow K_S^0 K^+ \pi^-) = (7.3 \pm 1.8) \times 10^{-4}$ and $\mathcal{B}(h_c \rightarrow K_S^0 K^+ \pi^-) \times \mathcal{B}(\psi(3686)) = (5.3 \pm 1.3) \times 10^{-7}$ with statistical uncertainties only.

IV. SYSTEMATIC UNCERTAINTIES

The sources of systematic uncertainties in the branching fraction measurement are tracking and PID efficiencies, reconstruction of photons, π^0 and K_S^0 , $K^+ \pi^0$ mass ranges, mass resolution of the signal shape, the MC model, input values, and the fit method. All sources of systematic uncertainties, which are summarized in Table I, are treated as independent and summed in quadrature. The details of their estimation are discussed in the following.

Tracking efficiencies. The uncertainties of tracking efficiencies of the kaon and pion from the primary vertex are 1.0% per track [28] and are added linearly.

PID efficiency. The uncertainty of PID is studied with a $\psi(2S) \rightarrow K_S^0 K^\pm \pi^\mp \pi^0$ control sample. The sample is selected by reconstructing one K_S^0 with a stricter requirement $L/\Delta L > 20$ and one π^0 with the number of photons restricted to be two. The signal region is $0.12 < M(\gamma \gamma) < 0.14 \text{ GeV}/c^2$ and $487.6 < M(K_S^0) < 507.6 \text{ MeV}/c^2$, and the PID efficiency is defined as $N_{\text{PID}}/N_{\text{all}}$, where N_{PID} and N_{all} are the number of events in the signal region with

TABLE I. Summary of systematic uncertainties.

Source	Relative uncertainty (%)
Tracking	2.0
PID	2.1
Photon reconstruction	2.0
K_S^0 reconstruction	1.0
π^0 reconstruction	0.7
5C kinematic fit	0.9
MC model	4.9
$M(K^+ \pi^0)$ mass window	...
Mass resolution	4.4
Fit method	3.4
Number of $\psi(3686)$	0.5
$\mathcal{B}(\psi(3686))$	7.3
Sum	11.1

and without PID. The difference between the efficiencies of MC and data is taken as the systematic uncertainty.

Photon reconstruction. The uncertainty of photon reconstruction, which is 1.0% for each photon, was determined with a control sample of $J/\psi \rightarrow \rho^0 \pi^0, \rho^0 \rightarrow \pi^+ \pi^-, \pi^0 \rightarrow \gamma\gamma$ [29].

K_S^0 reconstruction. The difference of K_S^0 reconstruction between MC simulation and data was studied based on the control samples of $J/\psi \rightarrow K^*(892)^\pm K^\mp$, $K^*(892)^\pm \rightarrow K_S^0 \pi^\pm$, and $J/\psi \rightarrow \phi K_S^0 K^\pm \pi^\mp$ [30], and its related uncertainty is 1.0%.

π^0 reconstruction. The uncertainty of π^0 reconstruction is studied using $\psi(3686) \rightarrow K_S^0 K^+ \pi^- \pi^0$ reconstructed with and without a π^0 mass constraint (0.12, 0.15) GeV/ c^2 and with the events in the h_c signal range excluded. The difference of π^0 reconstruction efficiency between data and MC simulation gives a relative uncertainty of 0.7%.

Kinematic fit. A correction of the helix parameters of the charged tracks in the MC samples is applied to improve the consistency between MC simulation and data. The uncertainty is estimated as half of the difference of efficiency with and without the correction, as suggested in Ref. [31], resulting in an uncertainty of 0.9%.

MC model. Because of the limited knowledge of intermediate states in the h_c decays, alternative MC samples are generated including the intermediate state $K^*(892)$ with the fractions of neutral and charged channels constrained by isospin symmetry. The result is compared with that of the nominal phase space result, and the difference is treated as the systematic uncertainty.

Mass resolution. An alternative control sample, $\psi(3686) \rightarrow \pi^0 J/\psi, J/\psi \rightarrow K_S^0 K^\pm \pi^\mp$, is used to determine the parameters of the mass resolution function, and the fit is repeated with the alternative mass resolution function. The difference of the fit yields to the nominal value gives a systematic uncertainty of 4.4%.

$K^+ \pi^0$ mass window. To study the potential uncertainty arising from the $M(K^+ \pi^0)$ mass window, a test introduced in Ref. [32] is performed by varying the range of the mass window around its nominal width. The test statistic ξ is defined as $\xi = \frac{|\mathcal{B} - \mathcal{B}'|}{\sqrt{|\sigma^2 - \sigma'^2|}}$, where $\mathcal{B}(\sigma)$ and $\mathcal{B}'(\sigma')$ are the resulting branching fractions (uncertainties) of the nominal result and from varied mass windows, respectively. If the values of ξ show a trending behavior and exceed two, a systematic uncertainty is assigned. We find the values of ξ of the branching fraction are always less than two and show no trending behavior around the nominal mass window; therefore, the related uncertainty is negligible.

Fit method. The same test as described in the last paragraph is performed with respect to the fitting ranges, and the related systematic effect is proved to be negligible. For the background modeling, the shape for the smooth background is changed from an ARGUS function to a second-order Chebychev polynomial, and for the peaking

background, the normalization scale is varied according to the uncertainty of the world average value of the branching fraction $\psi(3686) \rightarrow \gamma \chi_{c2}, \chi_{c2} \rightarrow K_S^0 K^+ \pi^-$ [7]. The corresponding change of the result is taken as the systematic uncertainty.

Input values. The number of $\psi(3686)$ events is quoted from Ref. [9], and the related uncertainty is taken into account. For the input branching fractions, the uncertainties associated with $K_S^0 \rightarrow \pi^+ \pi^-$ and $\pi^0 \rightarrow \gamma\gamma$ are negligible, and the uncertainty of $\psi(3686) \rightarrow \pi^0 h_c$ is assigned according to Ref. [8].

The signal significance is reestimated after considering alternative $M(K^+ \pi^0)$ mass windows, mass resolution parameters, fitting ranges, and background shape. Among these tests, the lowest significance, 4.3σ , is taken as the final signal significance.

V. SUMMARY AND DISCUSSION

Based on $(2.712 \pm 0.014) \times 10^9$ $\psi(3686)$ events collected at $\sqrt{s} = 3.686$ GeV with the BESIII detector, evidence of the hadronic decay $h_c \rightarrow K_S^0 K^+ \pi^-$ is found with a significance of 4.3σ after taking the systematic uncertainties into account. The product branching fraction $\mathcal{B}(\psi(3686) \rightarrow \pi^0 h_c) \times \mathcal{B}(h_c \rightarrow K_S^0 K^+ \pi^- + \text{c.c.})$ is $(5.3 \pm 1.3 \pm 0.4) \times 10^{-7}$, and the branching fraction $\mathcal{B}(h_c \rightarrow K_S^0 K^+ \pi^- + \text{c.c.})$ is determined to be $(7.3 \pm 1.8 \pm 0.8) \times 10^{-4}$, where the first and second uncertainties are statistical and systematic, respectively. Compared to the previous study by BESIII [6], in which an upper limit of $\mathcal{B}(\psi(3686) \rightarrow \pi^0 h_c) \times \mathcal{B}(h_c \rightarrow K_S^0 K^+ \pi^- + \text{c.c.}) < 4.8 \times 10^{-7}$, $CL = 90\%$ is obtained based on 4.48×10^8 $\psi(3686)$ events, our result is consistent.

Assuming that isospin symmetry holds in the decay of $h_c \rightarrow K \bar{K} \pi$, the ratios between isospin multiplets are $\mathcal{B}(h_c \rightarrow K^0 K^- \pi^+) : \mathcal{B}(h_c \rightarrow \bar{K}^0 K^+ \pi^-) : \mathcal{B}(h_c \rightarrow K^+ K^- \pi^0) : \mathcal{B}(h_c \rightarrow K^0 \bar{K}^0 \pi^0) = 2 : 2 : 1 : 1$. Combining with $\mathcal{B}(K^0 \rightarrow K_S^0) = 0.5$, we get the branching fraction $\mathcal{B}(h_c \rightarrow K \bar{K} \pi) = 3 \times \mathcal{B}(h_c \rightarrow K_S^0 K^+ \pi^- + \text{c.c.}) = (0.22 \pm 0.06)\%$, which is listed in Table II. Our result is consistent with the

TABLE II. Comparison between the theoretical predictions and the measurement of this work. Both statistical and systematic uncertainties are included.

Item	Value (%)	Source
$\mathcal{B}(h_c \rightarrow K \bar{K} \pi)$	1.4 ± 0.9	pQCD [4]
$\mathcal{B}(h_c \rightarrow K \bar{K} \pi)$	5.5 ± 3.3	NRQCD [4]
$\mathcal{B}(h_c \rightarrow K \bar{K} \pi)$	0.22 ± 0.06	This work
$\Gamma(h_c \rightarrow 3g) / \Gamma(\eta_c \rightarrow 2g)$	1.0 ± 0.1	pQCD [4]
$\Gamma(h_c \rightarrow 3g) / \Gamma(\eta_c \rightarrow 2g)$	8.3 ± 1.8	NRQCD [4]
$\Gamma(h_c \rightarrow 3g) / \Gamma(\eta_c \rightarrow 2g)$	0.93 ± 0.54	Refs. [7,33]
$\Gamma(h_c \rightarrow K \bar{K} \pi) / \Gamma(\eta_c \rightarrow K \bar{K} \pi)$	0.069 ± 0.062	This work

predictions based on pQCD and NRQCD, within 1.3 and 1.6 times the uncertainties, respectively.

Because the uncertainties of theoretical prediction are mainly caused by the input branching fractions of η_c , the comparison is rearranged by checking the following relation [34,35], which is used for calculating the exclusive branching fractions in Ref. [4],

$$\frac{\Gamma(h_c \rightarrow h)}{\Gamma(\eta_c \rightarrow h)} \approx \frac{\Gamma(h_c \rightarrow 3g)}{\Gamma(\eta_c \rightarrow 2g)}, \quad (2)$$

where h is any exclusive hadronic channel and $\Gamma(h_c \rightarrow 3g)$ and $\Gamma(\eta_c \rightarrow 2g)$ are the inclusive gluonic annihilation widths of h_c and η_c , respectively. While the theoretical uncertainties for the right-hand side of Eq. (2) are small, an estimation is also made as follows based on experimental results. Taking $\Gamma(h_c \rightarrow 3g) \approx \Gamma(h_c) \times (1 - \mathcal{B}(h_c \rightarrow \gamma\eta_c)) \approx 0.30 \pm 0.17$ MeV by neglecting all other radiative channels of h_c , and $\Gamma(\eta_c \rightarrow 2g) \approx \Gamma(\eta_c) \approx 32.0 \pm 0.7$ MeV by assuming a negligible radiative partial width of η_c , the ratio in the right-hand side of Eq. (2) is $\frac{\Gamma(h_c \rightarrow 3g)}{\Gamma(\eta_c \rightarrow 2g)} \approx (0.93 \pm 0.54)\%$, which is in good agreement with the pQCD prediction ($1.0 \pm 0.1\%$) but much smaller than the NRQCD prediction of $(8.3 \pm 1.8)\%$ [4]. Using the result from this work and the result from a global fit of η_c branching fractions [33] as inputs, we determine the ratio of partial widths $\frac{\Gamma(h_c \rightarrow K\bar{K}\pi)}{\Gamma(\eta_c \rightarrow K\bar{K}\pi)} = (0.069 \pm 0.062)\%$, where the central value differs from the right-hand side of Eq. (2) by 1 order of magnitude.

As a consequence, the test with Eq. (2) using our result for $\Gamma(h_c \rightarrow K\bar{K}\pi)/\Gamma(\eta_c \rightarrow K\bar{K}\pi)$, which is more sensitive than that of $\mathcal{B}(h_c \rightarrow K\bar{K}\pi)$, indicates inconsistencies with both pQCD and NRQCD predictions. Given that the predictions of the theoretical models have large uncertainties and only leading-order formulas for both pQCD and NRQCD are implemented, to resolve the gap between theoretical predictions and experimental measurements, refined predictions are required with improved precision and involving high-order effects such as corrections of renormalization scale [36] or relativistic effects [37]. On the other hand, the precision of our measurement is still strongly limited by statistical uncertainty, preventing us from drawing a solid conclusion.

ACKNOWLEDGMENTS

The BESIII Collaboration thanks the staff of BEPCII and the IHEP computing center for their strong support. This work is supported in part by National Key R&D Program of China under Contracts No. 2020YFA0406300, No. 2020YFA0406400, and No. 2023YFA1606000; National Natural Science Foundation of China (NSFC) under Contracts No. 11635010, No. 11735014, No. 11835012, No. 11935015, No. 11935016, No. 11935018, No. 11961141012, No. 12025502, 12035009, No. 12035013, No. 12061131003, No. 12192260, No. 12192261, No. 12192262, No. 12192263, No. 12192264, No. 12192265, No. 12221005, No. 12225509, and No. 12235017; the Chinese Academy of Sciences (CAS) Large-Scale Scientific Facility Program; the CAS Center for Excellence in Particle Physics (CCEPP); Joint Large-Scale Scientific Facility Funds of the NSFC and CAS under Contract No. U1832207; CAS Key Research Program of Frontier Sciences under Contracts No. QYZDJ-SSW-SLH003 and No. QYZDJ-SSW-SLH040; 100 Talents Program of CAS; The Institute of Nuclear and Particle Physics (INPAC) and Shanghai Key Laboratory for Particle Physics and Cosmology; European Union's Horizon 2020 research and innovation programme under Marie Skłodowska-Curie grant agreement under Contract No. 894790; German Research Foundation DFG under Contract No. 455635585, Collaborative Research Center CRC 1044, FOR5327, GRK 2149; Istituto Nazionale di Fisica Nucleare, Italy; Ministry of Development of Turkey under Contract No. DPT2006K-120470; National Research Foundation of Korea under Contract No. NRF-2022R1A2C1092335; National Science and Technology fund of Mongolia; National Science Research and Innovation Fund (NSRF) via the Program Management Unit for Human Resources & Institutional Development, Research and Innovation of Thailand under Contract No. B16F640076; Polish National Science Centre under Contract No. 2019/35/O/ST2/02907; The Swedish Research Council; and the U.S. Department of Energy under Contract No. DE-FG02-05ER41374.

-
- [1] D. J. Gross and F. Wilczek, *Phys. Rev. Lett.* **30**, 1343 (1973).
 [2] H. D. Politzer, *Phys. Rev. Lett.* **30**, 1346 (1973).
 [3] D. J. Gross and F. Wilczek, *Phys. Rev. D* **8**, 3633 (1973).
 [4] Y. Kuang, *Phys. Rev. D* **65**, 094024 (2002).
 [5] M. Ablikim *et al.* (BESIII Collaboration), *Phys. Rev. D* **99**, 072008 (2019).

- [6] M. Ablikim *et al.* (BESIII Collaboration), *Phys. Rev. D* **102**, 112007 (2020).
 [7] R. L. Workman *et al.* (Particle Data Group), *Prog. Theor. Exp. Phys.* **2022**, 083C01 (2022).
 [8] M. Ablikim *et al.* (BESIII Collaboration), *Phys. Rev. D* **106**, 072007 (2022).
 [9] M. Ablikim *et al.* (BESIII Collaboration), *arXiv:2403.06766*.

- [10] M. Ablikim *et al.*, Nucl. Instrum. Methods Phys. Res., Sect. A **614**, 345 (2010).
- [11] C. Yu *et al.*, in *Proceedings of the International Particle Accelerator Conference (IPAC'16), Busan, Korea, 2016*, International Particle Accelerator Conference No. 7 (JACoW, Geneva, Switzerland, 2016), pp. 1014–1018, 10.18429/JACoW-IPAC2016-TUYA01.
- [12] M. Ablikim *et al.*, Chin. Phys. C **44**, 040001 (2020).
- [13] J. Lu, Y. Xiao, and X. Ji, Radiat. Detect. Technol. Methods **4**, 1 (2020).
- [14] J. Zhang *et al.*, Radiat. Detect. Technol. Methods **6**, 289 (2022).
- [15] X. Li *et al.*, Radiat. Detect. Technol. Methods **1**, 13 (2017).
- [16] Y. Guo *et al.*, Radiat. Detect. Technol. Methods **1**, 15 (2017).
- [17] P. Cao *et al.*, Nucl. Instrum. Methods Phys. Res., Sect. A **953**, 163053 (2020).
- [18] S. Agostinelli *et al.*, Nucl. Instrum. Methods Phys. Res., Sect. A **506**, 250 (2003).
- [19] S. Jadach, B. F. L. Ward, and Z. Was, Phys. Rev. D **63**, 113009 (2001).
- [20] D. J. Lange, Nucl. Instrum. Methods Phys. Res., Sect. A **462**, 152 (2001).
- [21] R. Ping, Chin. Phys. C **32**, 599 (2008).
- [22] R. Yang, R. Ping, and H. Chen, Chin. Phys. Lett. **31**, 061301 (2014).
- [23] J. C. Chen, G. S. Huang, X. R. Qi, D. H. Zhang, and Y. S. Zhu, Phys. Rev. D **62**, 034003 (2000).
- [24] E. R. Was, Phys. Lett. B **303**, 163 (1993).
- [25] G. Punzi, eConf C **030908**, MODT002 (2003).
- [26] H. Albrecht *et al.*, Phys. Lett. B **241**, 278 (1990).
- [27] S. S. Wilks, Ann. Math. Stat. **9**, 60 (1938).
- [28] M. Ablikim *et al.* (BESIII Collaboration), Phys. Rev. D **83**, 112005 (2011).
- [29] M. Ablikim *et al.* (BESIII Collaboration), Phys. Rev. D **81**, 052005 (2010).
- [30] M. Ablikim *et al.* (BESIII Collaboration), Phys. Rev. D **92**, 112008 (2015).
- [31] M. Ablikim *et al.* (BESIII Collaboration), Phys. Rev. D **87**, 012002 (2013).
- [32] R. Barlow, arXiv:hep-ex/0207026.
- [33] H. Wang and C. Yuan, Chin. Phys. C **46**, 071001 (2022).
- [34] G. Chen and Y. Yi, Phys. Rev. D **46**, 2918 (1992).
- [35] Y. Kuang, S. F. Tuan, and T. Yan, Phys. Rev. D **37**, 1210 (1988).
- [36] Q. Zhang *et al.*, Chin. Phys. Lett. **31** (2014).
- [37] J. Li, Y.-Q. Ma, and K.-T. Chao, Phys. Rev. D **88**, 034002 (2013).